Classification of Normal and Abnormal Lungs with Interstitial Diseases by Rule-Based Method and Artificial Neural Networks

Shigehiko Katsuragawa, Kunio Doi, Heber MacMahon, Laurence Monnier-Cholley, Takayuki Ishida, and Takeshi Kobayashi

We devised an automated classification scheme by using the rule-based method plus artificial neural networks (ANN) for distinction between normal and abnormal lungs with interstitial disease in digital chest radiographs. Four measures used in the classification scheme are determined from the texture and geometric-pattern feature analyses. The rms variation and the first moment of the power spectrum of lung patterns are determined as measures for the texture analysis. In addition, the total area of nodular opacities and the total length of linear opacities are determined as measures for the geometric-pattern feature analysis. In our classification scheme with these measures, we identify obviously normal and abnormal cases first by the rule-based method and then ANN is applied for the remaining difficult cases. The rule-based plus ANN method provided a sensitivity of 0.926 at the specificity of 0.900, which was considerably improved compared to performance of either the rule-based method alone or ANNs alone.

KEY WORDS: computer-aided diagnosis, interstitial lung disease, automated classification, chest radiography.

EVALUATION OF INTERSTITIAL diseases in chest radiographs is considered one of the most difficult problems in diagnostic radiology, probably because of differences among radiologists in the terms that they use to identify interstitial infiltrates involving numerous patterns and complex variations.[1] The great proliferation of descriptive adjectives used produces considerable variations in interpretation among radiologists and institutions.[2] Computer-aided diagnosis (CAD),[3-5] which refers to a diagnosis made by a radiologist taking into consideration the results of an automated computer analysis of radiographic images, may improve the accuracy and overall reproducibility of interpretation of interstitial disease when the computer output is used as a "second opinion." Many investigators have attempted to develop CAD schemes for detection and characterization of interstitial lung diseases in chest radiographs.[6-10]

We have been developing computerized schemes for detection and characterization of interstitial disease in digital chest radiographs by using texture analysis,[11-16] based on the Fourier transform, and by geometric-pattern feature analysis,[17] based on filtering techniques. In texture analysis, the rms variation and the first moment of the power spectrum of lung patterns are determined as texture measures. In geometric-pattern feature analysis, the total area of nodular opacities and the total length of linear opacities are determined as geometric-pattern measures. The texture measures can represent overall features of lung texture, and they have been very useful in distinguishing between normal and abnormal lungs with interstitial disease, as reported previously.[11] On the other hand, the geometric-pattern measures can represent features related to the shape and size of individual opacities. Therefore, the combined analysis of texture and geometric-pattern measures has the potential to improve the distinction between normal and abnormal lungs with interstitial disease.

We previously reported[11] on the classification performance based on texture analysis with a rule-based method, which employs the number of abnormal regions of interest (ROIs) with large texture measures above a threshold value. Artificial neural networks (ANNs) have been used in many fields as a powerful classification tool in recent years.[18-21] In this study, we devised an automated classification scheme with the rule-based plus ANN method, using the combined analysis of texture measures and geometric-pattern measures for distinction between normal lungs and abnormal lungs with interstitial disease. In addition, we compared the classification performance among the rule-based method alone, an ANN method alone, and a rule-based plus ANN method.

From the Department of Radiology, Iwate Medical University, Morioka, Japan; the Kurt Rossmann Laboratories for Radiologic Image Research, Department of Radiology, The University of Chicago, Chicago, IL; Service de Radiologie, Hôpital Saint-Antoine, Paris, France; and the Department of Radiology, Kanazawa University, Kanazawa, Japan.

This study was supported by USPHS Grant CA 24806 and 62625.

Address reprint requests to Kunio Doi, PhD, Department of Radiology, The University of Chicago, 5841 South Maryland Ave, Chicago, IL 60637.

0897-1889/97/1003-0003$3.00/0

METHOD AND MATERIALS

Database of Chest Radiographs with Interstitial Disease

In order to establish a classification method, we created a database consisting of 200 conventional posteroanterior (PA) chest radiographs which were exposed with OC films and Lanex medium screens (Eastman Kodak Co, Rochester, NY). Our database included 100 normal lungs and 100 abnormal lungs with interstitial disease, which were selected based on consensus of independent review on each radiograph by four experienced chest radiologists. Normal cases were selected based on unequivocally normal radiographs and clinical data showing no clinically suspected cardiopulmonary disease. Abnormal cases with interstitial disease, which ranged from subtle to severe, were also selected based on radiographic findings, clinical data, and follow-up chest radiographs. The severity of interstitial infiltrates was subjectively evaluated by consensus of two radiologists. The number of cases in three categories (subtle, mild, and severe) were 15, 51, and 34, respectively. All chest radiographs included in the database were digitized with a laser scanner with a 0.175-mm pixel size and 1,024 gray levels.

Texture and Geometric-Pattern Feature Analyses

The overall scheme of the texture analysis is described later. Approximately 200 to 500 ROIs with a 32 × 32 matrix size are selected automatically in peripheral lung regions for each chest image.[15] The nonuniform background trend in each ROI is corrected for fluctuating patterns of the underlying lung texture.[11] The power spectrum of the lung texture is then obtained from the Fourier transform and is filtered by the visual system response of the human observer to suppress low frequency components caused by residual background trend and high frequency components attributable to radiographic mottle.[22] Finally, the rms variation in terms of relative exposure (R) and the first moment of the power spectrum (M) are determined as texture measures representing the magnitude and coarseness (or fineness) of the lung texture. R and M are defined as follows:

$$R = \frac{1}{G \cdot C \cdot (\log_{10} e)} \sqrt{\int_{-\infty}^{\infty}\int_{-\infty}^{\infty} V^2(u,v)\,|F(u,v)|^2\,du\,dv}$$

$$M = \frac{\int_{-\infty}^{\infty}\int_{-\infty}^{\infty} \sqrt{u^2+v^2}\,V^2(u,v)\,F(u,v)^2\,du\,dv}{\int_{-\infty}^{\infty}\int_{-\infty}^{\infty} V^2(u,v)\,|F(u,v)|^2\,du\,dv}$$

where G, C, $V(u,v)$, and $F(u,v)$, correspond to the gradient of the film used, the slope of the characteristic curve of the laser scanner,[16] the visual system response of the human observer, and the Fourier transform of lung textures, respectively. The factor $\log_{10} e$ is a conversion factor from the natural logarithm to the base 10 logarithm. The distribution of the two texture measures obtained for the normal and abnormal lungs included in our database is shown in Figure 1A. Only about 5% of all data were plotted because the total number of ROIs for the 100 normal and 100 abnormal cases is approximately 75,000.

In the geometric-pattern feature analysis, approximately forty ROIs with 128 × 128 matrix size are automatically selected in peripheral lung regions in the same method as that used for texture analysis.[15] It is known that interstitial infiltrates in chest images are composed basically of nodular and linear opacities.

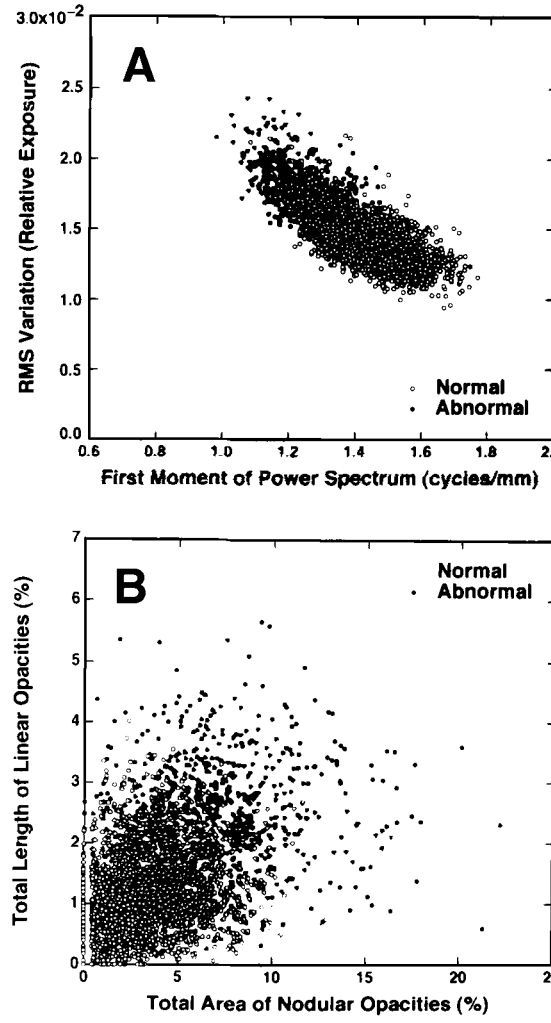

Fig 1. (A) Distribution of texture measures and (B) geometric-pattern measures obtained from 100 normal and 100 abnormal lungs with interstitial disease included in our database. For simplicity, only about 5% and 50% of all data are plotted for the texture measures and geometric-pattern measures, respectively.

Therefore, nodular and linear opacities of interstitial infiltrates are identified independently from two processed images, one of which is obtained by use of a multilevel thresholding technique and the other by use of a line enhancement filter. Finally, the total area of nodular opacities (A) and the total length of linear opacities (L) in each ROI are determined as geometric-pattern measures.[17] The distribution of the two geometric-pattern measures for normal and abnormal lungs is shown in Figure 1B. For simplicity, only about 50% of all data were plotted.

Normalization of Texture and Geometric-Pattern Measures

In general, normalization of measures based on the average and the standard deviation is useful for quantitative evaluation of different types of measures. Therefore, for subsequent

computerized classification, the texture and geometric-pattern measures obtained from a given chest image are normalized by means of the average and the standard deviation of these measures as determined for normal lungs that are included in the database as follows:

$$R_N = (R - \overline{R})/\sigma_R$$

$$M_N = (M - \overline{M})/\sigma_M$$

$$A_N = (A - \overline{A})/\sigma_A$$

$$L_N = (L - \overline{L})/\sigma_L$$

where R_N, M_N, A_N, and L_N are the normalized rms variation, the normalized first moment of the power spectrum, the normalized total area of nodular opacities, and the normalized total length of linear opacities, respectively; $\overline{R}$, $\overline{M}$, $\overline{A}$ and $\overline{L}$ are the average values of these measures for normal lungs; and ς_R, ς_M, ς_A and ς_L are the standard standard deviations of these measures for normal lungs.

The distributions of the normalized texture measures for normal and abnormal lungs included in the database are shown in Figure 2A. The distribution for normal lungs is centered around the origin, whereas the distribution for abnormal lungs is shifted to the upper left. There is a considerable overlap between the two distributions, however, because lung textures in abnormal lungs can comprise some normal areas unless interstitial infiltrates are spread over the entire lung.

The distributions of the normalized geometric-pattern measures for normal and abnormal lungs are shown in Figure 2B. The distribution for normal lungs is also centered around the origin, whereas the distribution for abnormal lungs is shifted to the upper right. There is again a considerable overlap between the two distributions. These overlaps indicate that a classification scheme based only on these distributions would not be very effective for distinction between normal and abnormal lungs with interstitial disease.

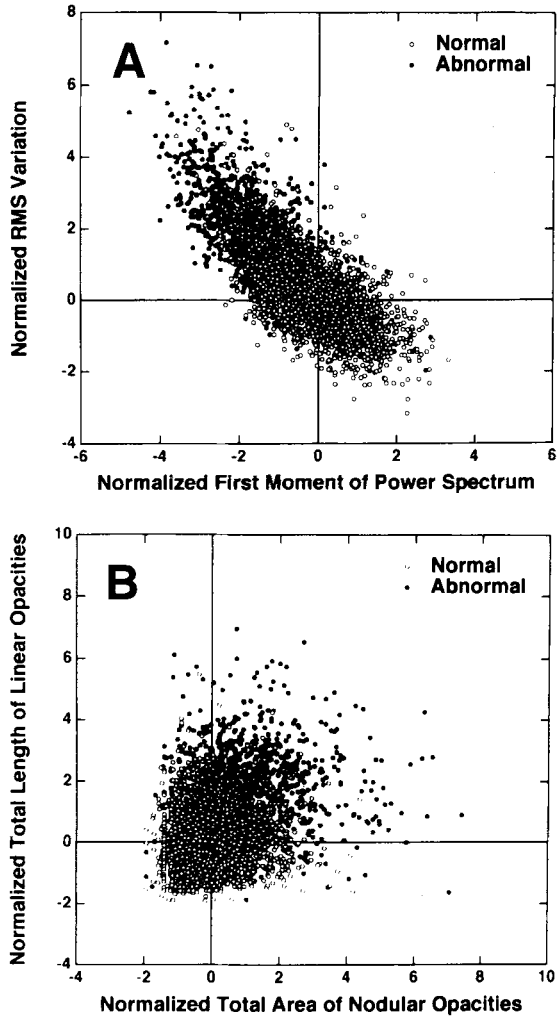

Fig 2. (A) Distribution of normalized texture measures and (B) normalized geometric-pattern measures. For simplicity, only about 5% and 50% of all data are plotted for the texture measures and geometric-pattern measures, respectively.

Single Texture and Geometric-Pattern Indices

As shown in Figure 2, the normalized texture and geometric-pattern measures for abnormal lungs are distributed widely. Typical abnormal patterns of interstitial infiltrates such as nodular, reticular, and reticulonodular patterns, however, can be characterized by distinct features. In the texture analysis, a nodular pattern has a low first moment of the power spectrum, a reticular pattern has a large rms variation, and a reticulonodular pattern has a large rms variation and a low first moment of the power spectrum.[11] In the geometric-pattern feature analysis, a nodular pattern has a large total area of nodular opacities, a reticular pattern has a large total length of linear opacities, and a reticulonodular pattern has a large total area of nodular opacities and a large total length of linear opacities.[17] Therefore, in order to facilitate the computerized classification, we determine a single texture index (T) and a single geometric-pattern index (G) from the two normalized texture measures and the two normalized geometric-pattern measures, respectively.

The single texture index (Fig 3) is defined as follows.[19]

$$T = R_N \quad \text{for } M_N > 0 \text{ and } R_N > 0$$

$$T = \sqrt{M_N^2 + R_N^2} \quad \text{for } M_N < 0 \text{ and } R_N > 0$$

$$T = -M_N \quad \text{for } M_N < 0 \text{ and } R_N < 0$$

$$T = -|Min(M_n, R_N)| \quad \text{for } M_N \geq 0 \text{ and } R_N \leq 0$$

The single geometric-pattern index is also defined in a similar fashion as follows:

$$G = L_N \quad \text{for } A_N < 0 \text{ and } L_N > 0$$

$$G = \sqrt{A_N^2 + L_N^2} \quad \text{for } A_N > 0 \text{ and } L_N > 0$$

$$G = -A_N \quad \text{for } A_N > 0 \text{ and } L_N < 0$$

$$G = Max(A_N, L_N) \quad \text{for } A_N \leq 0 \text{ and } L_N \leq 0$$

These single texture and geometric-pattern indices basically correspond to a distance from the average measures for normal lungs, as shown in Figure 3. We applied classification schemes with a rule-based method alone, an ANN method alone, and a

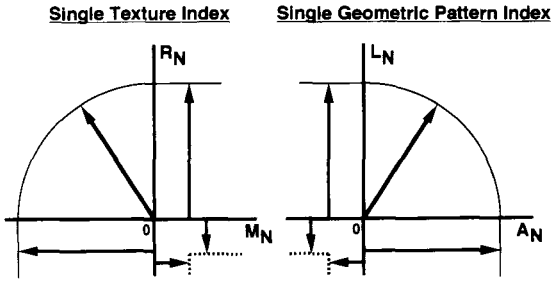

Fig 3. Definition of the texture index (left) and the geometric-pattern index (right). The texture and geometric-pattern indices (arrows) basically correspond to a distance from the average measures for normal lungs.

rule-based plus ANN method in which single texture indices and/or single geometric-pattern indices are used.

Rule-Based Method

For the rule-based method, we determine the number of suspicious abnormal ROIs that contain a single index greater than a threshold index. Then, if the ratio of the number of abnormal ROIs to the total number of ROIs selected in a chest image is greater than a threshold ratio, the chest image is classified as abnormal with interstitial disease.[11] In the rule-based methods in which either texture measures or geometric-pattern measures are used, the texture index or the geometric-pattern index is used as a single index. In the rule-based method in which the combined analysis of texture and geometric-pattern measures is used, an abnormal lung is classified by the logical OR operation, ie, if a chest image can be classified as abnormal *either* by texture measures *or* geometric-pattern measures, the chest image is finally classified as abnormal.

Artificial Neural Networks (ANN) Method

We also applied artificial neural networks (ANNs) for classification of normal and abnormal lungs with interstitial diseases. In this study, three-layer, feed-forward networks with a back-propagation algorithm[23] were employed. The structure of the ANN includes three hidden units and one output unit, which represents the classification result (0 = normal, 1 = abnormal). The input data for the ANN are selected from a histogram of the single-texture indices and/or that of the geometric-pattern indices. For the ANN with texture measures, the histogram of the single-texture indices is determined for each chest image, as shown in Figure 4. Then, five input values for the ANN, X_1-X_5 in Figure 4, are selected from the corresponding single-texture indices at the upper 10%, 30%, 50%, 70%, and 90% areas of the histogram. For the ANN with geometric-pattern measures, five single geometric-pattern indices are selected as the input data for the ANN in a similar way. In addition, for the ANN with the combined analysis of texture and geometric-pattern measures, four single texture indices (at the upper 20%, 40%, 60%, and 80% area of the histogram) and three single geometric-pattern indices (at the upper 20%, 50%, and 80%) are selected as the input to the ANN.

Rule-Based Plus ANN Method

The overall scheme for classification with the rule-based plus ANN method is shown in Figure 5. First, the rule-based method

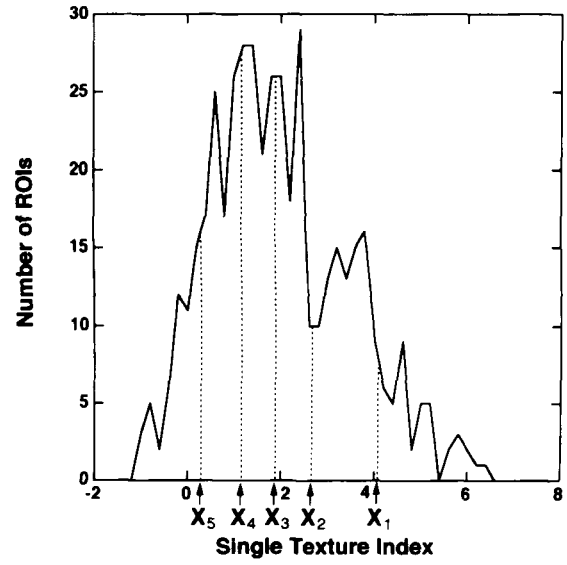

Fig 4. Histogram of texture indices obtained from a chest radiograph with interstitial infiltrates. Five input data for the ANN are texture indices X_1, X_2, X_3, X_4, and X_5 at upper ten, thirty, fifty, seventy, and ninety percent area of the histogram, respectively.

is employed for identification of obviously normal and obviously abnormal lungs. Then the ANN is applied for classification of the remaining chest images, which were not classified as obvious cases by the rule-based method.

For the rule-based plus ANN method based on either texture measures or geometric-pattern measures, a chest image is classified as "obviously" normal if the ratio of the number of

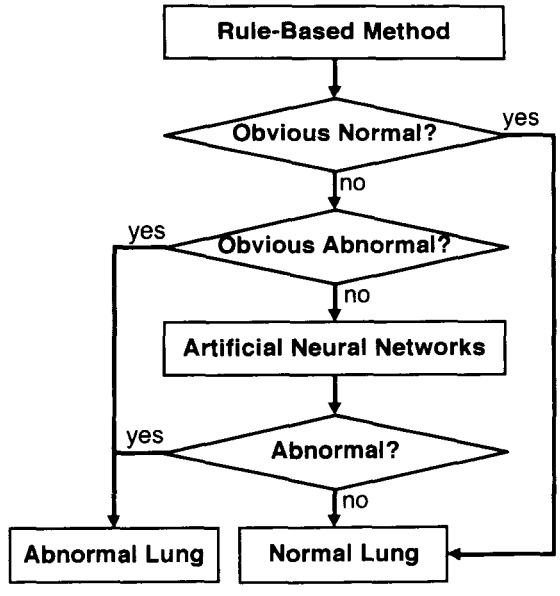

Fig 5. Overall classification scheme with the rule-based plus ANN method.

abnormal ROIs to the total number of ROIs in the chest image is below the minimum "abnormal" ratio that can be obtained from all abnormal cases in a training data set; however, the chest image is classified as "obviously" abnormal if the ratio is above the maximum "normal" ratio that can be obtained from all normal cases in the training data set. The minimum and maximum ratios used for classification of obvious cases are determined from a training data set, as will be discussed later.

For the rule-based plus ANN method with the combined analysis of texture and geometric-pattern measures, obvious cases are identified by logical AND operation (ie, if a chest image can be classified as normal by the initial rule-based method based on *both* texture measures *and* geometric-pattern measures, the chest image is classified as obviously normal). Obviously abnormal cases are classified in a similar way.

Evaluation of Classification Performance

For evaluation of the classification performance with various methods, the original database including 100 normal and 100 abnormal cases with interstitial disease was divided into two groups by use of random numbers. One is a data set for training, which includes 50 normal and 50 abnormal cases. Another is a data set for testing, which also includes 50 normal and 50 abnormal cases. We prepared 10 pairs of different training and testing data sets. For each pair of data sets, the normalizations of measures were achieved with the average and standard deviation of measures for normal lungs in each training data set.

For classification with the rule-based method, the threshold levels of the texture and/or the geometric-pattern indices are determined in such a way as to achieve the best classification performance for a given training data set. In the rule-based plus ANN method, the minimum ratio of the number of abnormal ROIs to the total number of ROIs for all abnormal cases and the maximum ratio of abnormal ROIs for all normal cases are also determined from a training data set. The internal parameters of the ANN are determined from more than 100 iterations of learning for a training data set, after obviously normals and obviously abnormals were eliminated by the initial rule-based method. These parameters are used for a validation test with a testing data set.

The classification performance is evaluated by receiver operating characteristic (ROC) analysis.[24] For classification with the rule-based method, ROC curves are obtained by changing the threshold level in terms of the ratio of the number of abnormal ROIs to the total number of ROIs. For classification with the ANN method, ROC curves are obtained by changing the threshold level in terms of the ANN output. Finally, the average classification performance for each method is determined by use of 10 different training-testing data sets. The statistical significance of differences between ROC curves is determined by application of a two-tailed paired *t* test to the Az value (the area under ROC curves) of each testing data set.

RESULTS AND DISCUSSION

Figure 6A shows ROC curves obtained for classification methods with texture measures with the rule-based method alone, the ANN method alone, and the rule-based plus ANN method. The Az value of 0.958 for the rule-based plus ANN method is larger than that of 0.947 for the rule-based method alone ($P < .05$) and 0.957 for the ANN method alone ($P < .20$). ROC curves obtained for various classification methods based on geometric pattern measures are shown in Figure 6B. The Az value of 0.943 for the rule-based plus ANN method is larger than that of 0.937 for the rule-based method alone ($P < .05$) and 0.941 for the ANN method alone ($P < .50$). In addition, ROC curves for the combined analysis of texture and geometric-pattern measures are shown in Figure 6C. The Az value of 0.966 for the rule-based plus ANN method is larger than that of 0.959 for the rule-based method alone ($P < .05$) and 0.965 for the ANN method alone ($P < .10$).

It should be noted that the rule-based plus ANN method always improves the classification performance compared with either the rule-based method alone or the ANN method alone and that the classification performance obtained with the ANN method alone is superior to that with the rule-based method alone. These results indicate that the overall classification performance is improved if the obvious (easy) cases are eliminated initially by the rule-based method and only the remaining uncertain (difficult) cases are classified by the ANN method. This is probably because difficult cases alone can be used more effectively in training of the ANN than all cases including easy cases, and thus this method yields improved performance.

Table 1 is a summary of the classification performance expressed by the sensitivity at the specificity of 0.900. Although the sensitivity obtained with the use of texture measures is higher than that for geometric-pattern measures, the combined analysis can improve the sensitivity in comparison with individual analyses for all classification methods. These results suggest that texture analysis and geometric-pattern feature analysis can complement each other. It should be noted that classification with the rule-based plus ANN method by use of the combined analysis of texture and geometric-pattern measures provides the best performance.

When the combined analysis of texture and geometric-pattern measures is used for classification with the rule-based methods, another logical operation can be applied. We tried using the logical AND operation in the rule-based method alone (ie, if a chest image could be classified as abnormal by the rule-based method with the use of *both* texture measures *and* geometric-pattern measures, the chest

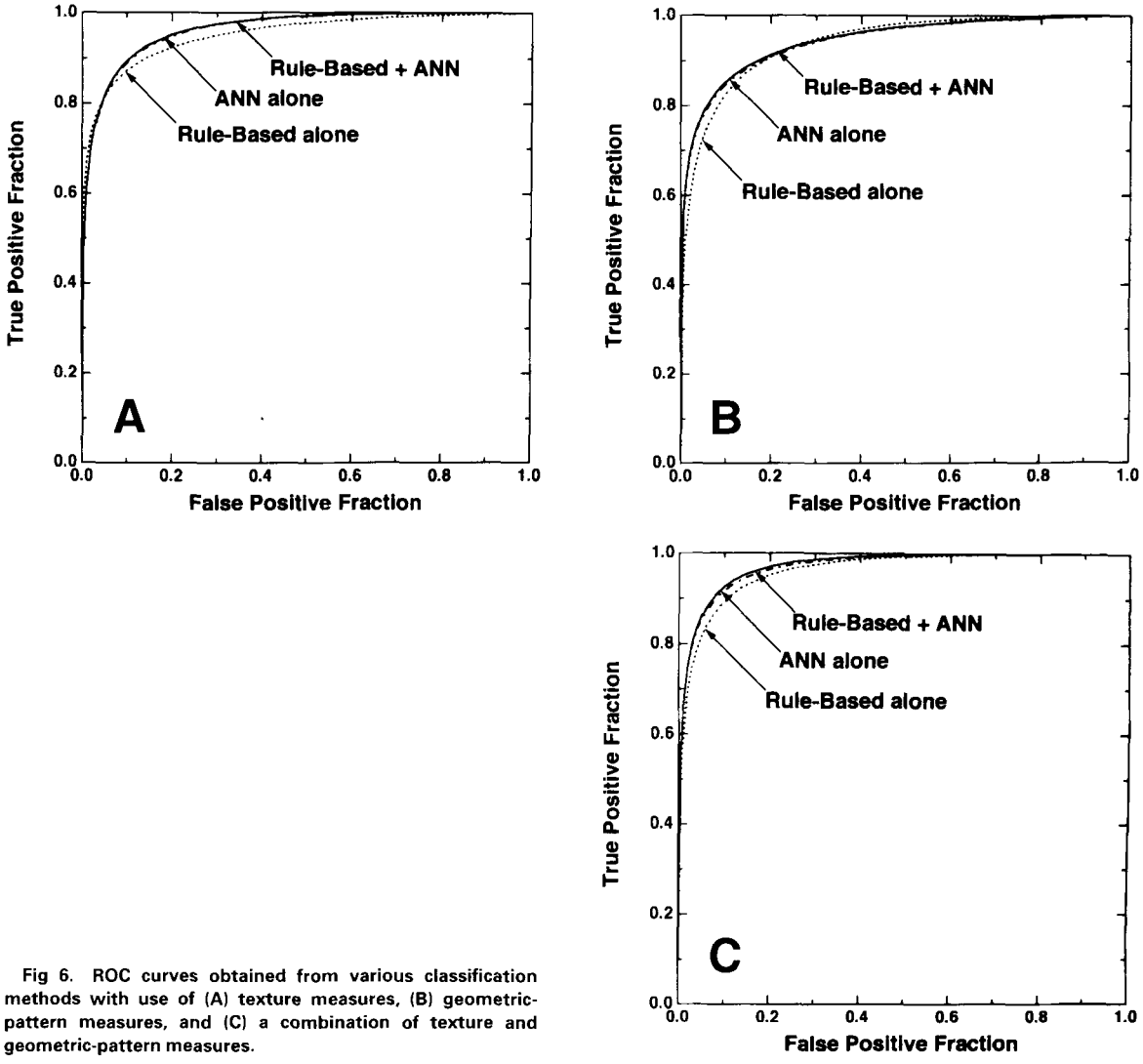

Fig 6. ROC curves obtained from various classification methods with use of (A) texture measures, (B) geometric-pattern measures, and (C) a combination of texture and geometric-pattern measures.

image was then classified as abnormal). The Az value obtained from the ROC curve was 0.947, and the sensitivity at the specificity of 0.900 was 0.865. This result indicates that the logical AND operation for combined analysis of measures in the rule-based method alone did not improve the classification performance, because the sensitivity obtained from geometric-pattern measures is considerably lower than that obtained from texture measures. In addition, we examined the logical OR operation for classification of obvious cases in the rule-based plus ANN method. If a chest image could be classified as obviously normal by the rule-based method with the use of *either* texture measures *or* geometric-pattern measures, the chest image was classified as obviously normal. A lung was also classified as obviously abnormal by the logical OR operation. The Az value was 0.954, and the sensitivity was 0.907. This result indicates that the logical OR operation for identification of obvious cases did not improve the overall classification performance in the rule-based plus ANN method. This is because the overall classification performance is affected by

Table 1. Sensitivity at the Specificity of 0.900 for Various Classification Schemes in Distinguishing Between Normal and Abnormal Lungs with Interstitial Disease

	Texture Measures	Geometric Pattern Measures	Combination
Rule-Based	0.873	0.826	0.893
ANN	0.890	0.848	0.917
Rule-Based + ANN	0.894	0.853	0.926

some false-positives and false-negatives which may be classified incorrectly as obvious cases because of the logical OR operation in the rule-based method. Therefore, it is very important to identify obvious cases conservatively and correctly in the initial rule-based method and then to classify the remaining difficult cases with the ANN method, when the rule-based plus ANN method is employed.

CONCLUSION

In summary, we devised a computerized classification scheme with the rule-based plus ANN method by using the combined analysis of texture measures and geometric-pattern measures for distinction between normal and abnormal lungs with interstitial disease. Because obvious cases are eliminated by the rule-based method, and uncertain difficult cases can be effectively classified by the ANN method, the overall classification performance can be improved. Therefore, the classification performance with the rule-based plus ANN method is superior to either that with the rule-based method alone or that with the ANN method alone. In addition, the combined analysis of texture measures and geometric-pattern measures can improve the classification performance in comparison with individual analysis. We believe that this computerized classification method can assist radiologists in the diagnosis of interstitial diseases in digital chest radiographs.

ACKNOWLEDGMENT

The authors are grateful to Xin-Wei Xu, PhD, for his participation in discussions on the computer scheme, E. Lanzl for editing the manuscript, and E.A. Ruzich for her secretarial work. Kunio Doi and Heber MacMahon are shareholders of R2 Technology, Inc, Los Altos, CA. It is the policy of the University of Chicago that investigators disclose publicly actual or potential significant financial interests that may appear to be affected by the research activities.

REFERENCES

1. Fraser RG, Pare JA: Diagnosis of Diseases of the Chest. Philadelphia, PA, Saunders, 1970

2. Tully RJ, Conners RW, Harlow CA, et al: Toward computer analysis of pulmonary infiltration. Invest Radio 13:298-305, 1978

3. Doi K, Giger ML, MacMahon H, et al: Computer-aided Diagnosis (CAD): Development of automated schemes for quantitative analysis of radiographic images. Semin Ultrasound CT MR 13:140-152, 1992

4. Giger ML, Doi K, MacMahon H, et al: An intelligent workstation for computer-aided diagnosis. RadioGraphics 13: 647-656, 1993

5. MacMahon H, Doi K, Chan HP, et al: Computer-aided diagnosis in chest radiology. J Thorac Imag 5:67-76, 1990

6. Jagoe JR, Paton KA: Reading chest radiographs by computer. Br J Ind Med 32:267-272, 1975

7. Revesz G, Kundel HL: Feasibility of classifying disseminated pulmonary diseases based on their Fourier spectra. Invest Radiol 8:345-349, 1973

8. Turner AF, Kruger RP, Thompson WB: Automated computer screening of chest radiographs for pneumoconiosis. Invest Radiol 11:258-266, 1976

9. Kruger RP, Thompson WB, Turner AF: Computer diagnosis of pneumoconiosis. IEEE Trans Syst Man Cybern 4:40-49, 1974

10. Kido S, Ikezoe J, Naito H, et al: An image analyzing system for interstitial lung abnormalities in chest radiography: Detection and classification by Laplacian-Gaussian filtering and linear opacity judgment. Invest Radiol 29:172-177, 1994

11. Katsuragawa S, Doi K, MacMahon H: Image feature analysis and computer-aided diagnosis in digital radiography: Detection and characterization of interstitial lung disease in digital chest radiographs. Med Phys 15:311-319, 1988

12. Powell GF, Doi K, Katsuragawa S: Localization of inter-rib spaces for lung texture analysis and computer-aided diagnosis in digital chest images. Med Phys 15:581-587, 1988

13. Katsuragawa S, Doi K, Nakamori N, et al: Image feature analysis and computer-aided diagnosis in digital radiography: Effect of digital parameters on the accuracy of computerized analysis of interstitial disease in digital chest radiographs. Med Phys 17:72-78, 1990

14. Katsuragawa S, Doi K, MacMahon H, et al: Quantitative computer-aided analysis of lung texture in chest radiographs. RadioGraphics 10:257-269, 1990

15. Chen X, Doi K, Katsuragawa S, et al: Automated selection of regions of interest for quantitative analysis of lung textures in digital chest radiographs. Med Phys 20:975-982, 1993

16. Morishita J, Doi K, Katsuragawa S, et al: Computer-aided diagnosis for interstitial infiltrates in chest radiographs: Analysis of optical-density dependence on texture measures. Med Phys 22:1515-1522, 1995

17. Katsuragawa S, Doi K, MacMahon H, et al: Quantitative analysis of geometric-pattern features of interstitial infiltrates in digital chest radiographs. J Digit Imaging 9:137-144, 1996

18. Asada N, Doi K, MacMahon H, et al: Potential usefulness of an artificial neural network for differential diagnosis of interstitial lung diseases: Pilot study. Radiology 177:857-860, 1990

19. Boone JM, Gross GW, Greco-Hunt V: Neural networks in radiologic diagnosis: I. Introduction and illustration. Invest Radiol 25:1012-1016, 1990

20. Wu Y, Doi K, Giger ML, et al: Computerized detection of clustered microcultifications in digital mammograms: Application of artificial neural networks. Med Phys 19:555-560, 1992

21. Wu Y, Giger ML, Doi K, et al: Artificial neural networks in mammography: Application to decision making in the diagnosis of breast cancer. Radiology 187:81-87, 1993

22. Chan HP, Metz CE, Doi K: Digital image processing: Optimal spatial filter for maximization of the perceived SNR based on a statistical decision theory model for the human observer. Proc SPIE 535:2-11, 1985

23. Rogers SK, Kabrisky M: An introduction to biological and artificial neural networks for pattern recognition. Bellingham, WA, SPIE Press, 1991

24. Metz CE: ROC methodology in radiologic imaging. Invest Radiol 21:720-733, 1986